Photocatalysis

DOI: 10.1002/ange.201207554

Photocatalytic Overall Water Splitting Promoted by an α–β phase Junction on Ga_2O_3**

*Xiang Wang, Qian Xu, Mingrun Li, Shuai Shen, Xiuli Wang, Yaochuan Wang, Zhaochi Feng, Jingying Shi, Hongxian Han, and Can Li**

Direct overall water splitting with semiconductor-based photocatalysts is one of the most ideal routes for hydrogen production using solar energy.[1,2] However, most of the semiconductor photocatalysts thus far investigated show only low activity for overall water splitting, the simultaneous splitting of water into H_2 and O_2. One of the key issues related to this problem is the limited charge separation efficiency upon photo-excitation, which largely depends on the intrinsic electronic and structural properties of semiconductors.[2] To improve the photocatalytic activity of overall water splitting, it is highly desirable to develop approaches that can efficiently promote charge separation in semiconductor based photocatalysts.[3] Fabrication of junctions (such as p–n junctions) between different semiconductors has been demonstrated to be an effective strategy for promoting charge separation in photovoltaics.[4] Proper junctions formed in semiconductor-based photocatalysts could also lead to enhanced activity in either hydrogen or oxygen half reactions.[5] However, fabricating efficient junctions for the overall water splitting reaction still remains a challenge. More importantly, the essential relation between the junction and the photocatalytic activity is far less well understood. An in-depth understanding of junction-related issues may be a great aid in the design and preparation of efficient semiconductor based photocatalysts.

Herein, we report that Ga_2O_3 with tuneable α–β phase junctions can stoichiometrically split water into H_2 and O_2 with drastically enhanced activity over those with α or β phase structures alone. The enhanced photocatalytic performance is shown to be due to efficient charge separation and transfer across the α–β phase junction. Rational design and fabrication of phase junctions is therefore demonstrated to be an attractive strategy for the development of efficient photocatalysts for overall water splitting.

Gallium oxide is an n-type semiconductor with five polymorph phases, including commonly seen α and β phases.[6] Ga_2O_3 semiconductors with different phase structures were prepared by phase transformation from α-Ga_2O_3 into β-Ga_2O_3 at elevated temperatures. The phase transformation was followed by XRD and UV Raman spectroscopy. As shown in Figure 1, both the XRD patterns and the UV Raman spectra suggest that the original α-Ga_2O_3 undergoes gradual α to β phase transformation upon increasing the calcination temperature from 673 to 1073 K, and Ga_2O_3 with different phase structures could be obtained during the phase transformation. However, some discrepancies are observed in the results between the UV Raman spectra and the XRD patterns for the samples obtained by the calcination of α-Ga_2O_3 at 863 and 903 K (denoted as Ga_2O_3-863 and Ga_2O_3-903, respectively) owing to the greater sensitivity of UV Raman spectroscopy to the outer region of the solid samples than XRD.[7] For Ga_2O_3-863, the presence of characteristic β-Ga_2O_3 bands in the UV Raman spectra[8] and the absence of characteristic β-Ga_2O_3 diffraction peaks in XRD indicate that β-Ga_2O_3 is formed in the outer region. For Ga_2O_3-903, the characteristic Raman bands of α-Ga_2O_3[9] disappear, whereas the characteristic diffraction peaks of α-Ga_2O_3 are still clearly detected by XRD, which indicates that the outer region of Ga_2O_3-903 is fully covered with β-Ga_2O_3 while maintaining an inner bulk region of α-Ga_2O_3 (see Figure S1 in the Supporting Information for more details). Overall, by finely tuning the phase transformation temperature in the range of 863–903 K,

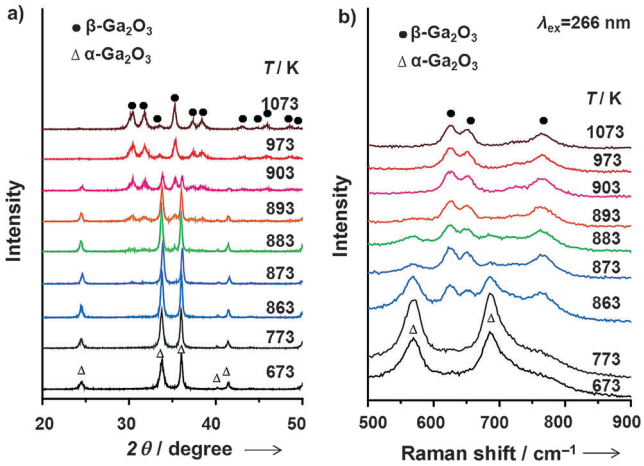

Figure 1. a) XRD patterns, and b) UV Raman spectra (excitation line at 266 nm) of different samples prepared by calcination of α-Ga_2O_3 at different temperatures for 1.5 h in air. The samples obtained by calcining α-Ga_2O_3 at 673 and 1073 K are α-Ga_2O_3 and β-Ga_2O_3, respectively, as determined by a comparison of the XRD patterns with the JCPDS card numbers 06-0503 and 41-1103.

[*] X. Wang, Dr. Q. Xu, Dr. M. Li, S. Shen, Dr. X. Wang, Dr. Y. Wang, Prof. Z. Feng, Dr. J. Shi, Prof. H. Han, Prof. C. Li
State Key Laboratory of Catalysis, Dalian Institute of Chemical Physics, Chinese Academy of Sciences, Dalian National Laboratory for Clean Energy, 457 Zhongshan Road, Dalian 116023 (China)
E-mail: canli@dicp.ac.cn
Homepage: http://www.canli.dicp.ac.cn

[**] This work was financially supported by the National Natural Science Foundation of China (21090341, 21061140361 and 20923001) and the Ministry of Science and Technology of China (2009CB220010).

Supporting information for this article is available on the WWW under http://dx.doi.org/10.1002/anie.201207554.

a series of Ga_2O_3 samples with different compositions of α-Ga_2O_3 and β-Ga_2O_3 have been prepared.

The phase structures of Ga_2O_3-863 and Ga_2O_3-903 were investigated by high resolution transmission electron microscopy (HRTEM). For Ga_2O_3-863, the images in Figure 2 a,b show that small β-Ga_2O_3 nanoparticles are sporadically

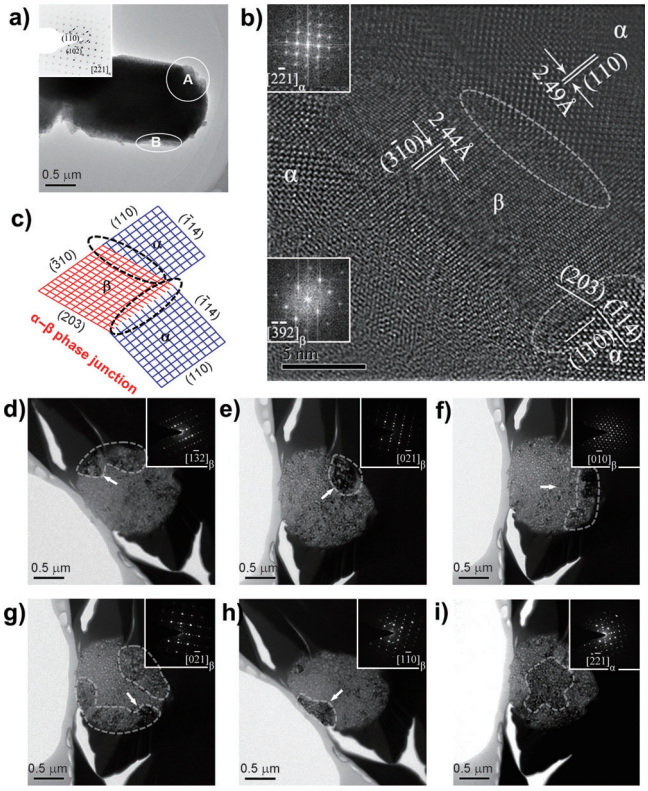

Figure 2. a) Low-magnification image of Ga_2O_3-863. The inset is the SAED pattern taken from area A, showing that area A contains both α and β phases. b) HRTEM image taken from area B in (a). c) A simplified cartoon depicting the α–β phase junctions according to (b). d)–i) TEM images taken at different tilt angles for one cross-section of a Ga_2O_3-903 particle. The insets are the corresponding SAED patterns. The areas in (d)–(h) and (i), which show darker contrast owing to satisfaction of the Bragg reflection condition, are identified as β-Ga_2O_3 and α-Ga_2O_3, respectively.

patched onto the surface of the original α-Ga_2O_3 particle, resulting in the exposure of both α and β phases on the surface. Moreover, it can be observed in Figure 2 b that the phase junction between α-Ga_2O and β-Ga_2O_3 is composed of well-matched lattice fringes between the (110) plane of α-Ga_2O_3 and the $(3\bar{1}0)$ plane of β-Ga_2O_3 with a lattice mismatch of only 3% (Figure 2 c). UV Raman and XRD also revealed that the surface of the Ga_2O_3-903 sample is fully covered by
β-Ga_2O_3, whereas the inner bulk is still α-Ga_2O_3. To confirm this phase structure, a randomly selected Ga_2O_3-903 particle was milled halfway through its thickness with a focused ion beam and the exposed cross section was characterized with TEM. As shown in Figure 2 d–i, an α/β core/shell structure with
α-Ga_2O_3 in the inner core and β-Ga_2O_3 in the surrounding shell is observed. This confirms that the phase transformation has been completed on the outer region of Ga_2O_3-903, resulting in the exposure of only β-Ga_2O_3 on the surface. Moreover, a well-structured α–β phase junction is also seen at the boundary of the α phase core and the β phase shell (Supporting Information, Figure S2). These observations clearly demonstrate that atomically well-defined α–β phase junctions of Ga_2O_3 can be tailor-designed and obtained by phase transformation.

The photocatalytic overall water splitting reactions were carried out on the different phase-structured Ga_2O_3-based photocatalysts, and the photocatalytic activities are shown in Figure 3. All of these photocatalysts can truly split water into H_2 and O_2 in a ratio of approximately 2:1. However, the

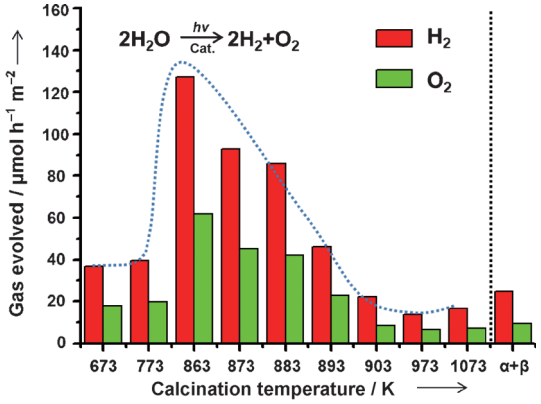

Figure 3. Specific H_2 and O_2 evolution activities (normalized by specific surface area) of α-Ga_2O_3 samples calcined at different temperatures as a comparison of their photocatalytic activity. The notation α + β indicates the mechanically mixed sample with a 1:1 ratio of α-Ga_2O_3/β-Ga_2O_3. For the photocatalytic reaction experiments, photocatalysts (0.5 g) loaded with NiO_x (2 wt%) co-catalyst were dispersed into deionized water (500 mL) and irradiated with a 450 W mercury lamp (USHIO UM452).

photocatalytic activities of these samples are quite different. The samples in the α phase (calcined from 673 to 773 K) or the β phase (calcined from 973 to 1073 K) alone have relatively low photocatalytic activities, whereas the samples prepared by the calcination of α-Ga_2O_3 at 863–893 K show much higher photocatalytic activity. Typically, the photocatalytic activity of Ga_2O_3-863 with both α and β phases exposed on the surface reaches up to three or seven-fold greater than that of α-Ga_2O_3 or β-Ga_2O_3 alone, respectively. Furthermore, the photocatalytic activity of Ga_2O_3-863 is much higher than that of mechanically mixed α-Ga_2O_3 and β-Ga_2O_3 samples, which is nearly equal to the simple sum of the activities of α-Ga_2O_3 and β-Ga_2O_3 alone. The different photocatalytic activities are not due to differences in particle size or surface area, as there are no distinct changes among these samples (Table S1). It is only the α–β phase junction formed between two different phases that is responsible for the considerable enhancement in the photocatalytic activity for overall water splitting.

One may notice that although the α–β phase junction is formed, the samples obtained by calcination of α-Ga_2O_3 at

temperatures above 863 K show lower photocatalytic activity relative to Ga_2O_3-863. Typically, Ga_2O_3-903 shows photocatalytic activity nearly as low as that of β-Ga_2O_3. From XRD and UV Raman spectroscopy, we know that the amount of β-Ga_2O_3 on the surface gradually increases as the calcination temperature increases. This leads to an α/β core/shell structure with only the β phase exposed on the Ga_2O_3-903 surface formed, whereas both α and β phases are exposed on the Ga_2O_3-863 surface. This suggests that the presence of the α–β phase junction and the exposure of both phases on the surface are essential for the enhancement of photocatalytic activity.

To further understand the role of α–β phase junctions in the photocatalytic reaction, the kinetics of photogenerated charge carriers in samples with different phase structures were investigated by ultra-fast transient absorption spectroscopy and time-resolved IR spectroscopy. As shown in Figure 4a, the α–β phase junction in Ga_2O_3-863 results in an ultrafast transfer at approximately 3 ps (see Table S2 for details). This ultrafast transfer is much faster than the recombination (> 1000 ps)[10] and the trap processes (14–32 ps),[11] which indicates a much more efficient charge separation for the Ga_2O_3-863 with the α–β phase junctions. Furthermore, the electron–hole recombination kinetics observed by time-resolved IR spectroscopy (Figure 4b) show that the lifetime of the long-lived photogenerated electrons in the microsecond time-scale for Ga_2O_3-863 with α–β phase junctions is much longer than those in either α-Ga_2O_3 or β-Ga_2O_3 alone. Such long-lived electrons are most likely responsible for the enhancement in the photocatalytic activity.[12]

It should be mentioned that not all long-lived charge carriers can contribute to the course of the photocatalytic reaction. Only those that reach the surface have an opportunity to participate in the surface reactions. A time-resolved in situ FT-IR experiment was specially conducted to probe the photogenerated holes on the surface of the Ga_2O_3 samples using methanol as electron donor. The initial IR absorption intensity, shown in Table 1, originates from the photogenerated electrons, and the increase in the IR absorption intensity after introducing methanol vapor onto the Ga_2O_3 sample is due to the capture of holes by methanol. There are two competition processes for the photogenerated holes, either recombination with photogenerated electrons or trapping by methanol on the surface. Therefore, the increase in the IR absorption intensity directly reflects the amount of the charges available on the surface for the photocatalytic reaction. Interestingly, Ga_2O_3-863, with α–β phase junctions, shows a larger increase in the initial IR absorption intensity than α-Ga_2O_3 and β-Ga_2O_3 samples, which suggests that there are more holes available to participate in the surface reaction on Ga_2O_3-863. These results further demonstrate that the α–β phase junctions in Ga_2O_3-863 can more effectively promote charge separation. As a consequence, more long-lived photogenerated charges contribute to the photocatalytic water splitting reaction.

The band structures of α-Ga_2O_3 and β-Ga_2O_3 were further examined by Mott–Schottky measurements and XPS. As shown in Figure 4c,d, the flat band potential of α-Ga_2O_3 is more negative than that of β-Ga_2O_3, and the valence band potential of β-Ga_2O_3 is more positive than that of α-Ga_2O_3. By further taking into account the band gaps (Figure S4), a band structure diagram of an α–β phase junction can be drawn (Figure 4e). Upon irradiation of Ga_2O_3 with α–β phase junctions, the photogenerated electrons tend to transfer from the α phase to the β phase, while the

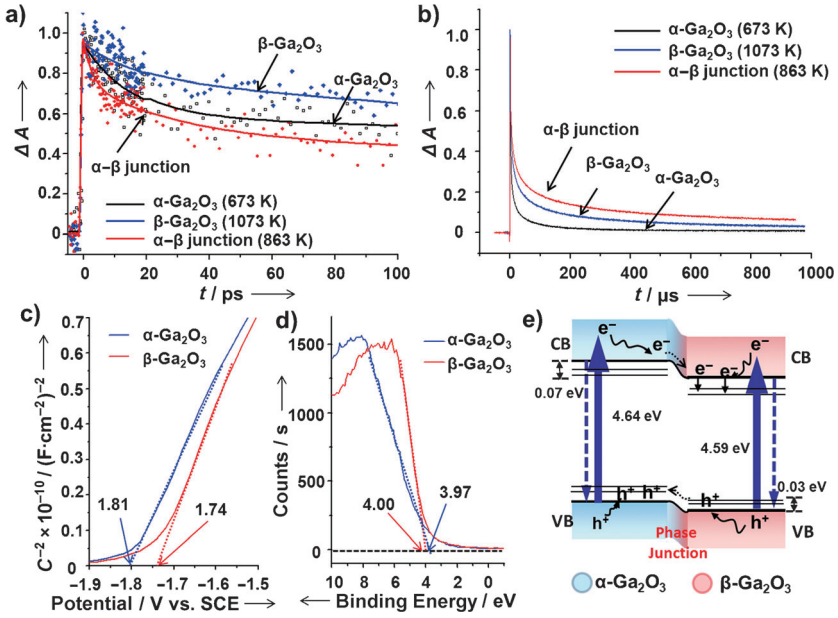

Figure 4. a) Normalized time profiles of transient absorption spectra at 850 nm of Ga_2O_3 samples excited by a 255 nm laser with a 50 fs pulse duration. b) Normalized transient absorption profiles of average mid-IR absorption of Ga_2O_3 samples excited by a 266 nm laser pulse of 6–8 ns duration; α–β junction: Ga_2O_3 with an α–β phase junction obtained by calcining an α-Ga_2O_3 sample at 863 K. c) Mott–Schottky curves of α-Ga_2O_3 and β-Ga_2O_3 electrodes measured in Na_2SO_4 solution (0.3 M, pH ca. 7.0). d) XPS valence band spectra of α-Ga_2O_3 and β-Ga_2O_3. e) Illustration of charge transfer cross the α–β phase junction.

Table 1: Time resolved in situ FT-IR absorptions of Ga_2O_3 samples with different phase structures.

Entry	Sample	Initial intensity		Increase in initial intensity	
		I_V[a]	I_C[b]	($I_C - I_V$)	I_C/I_V
1	α[c]	5.4	16	10.6	2.96
2	β[d]	90	101	11	1.12
3	α–β[e]	4.7	40	35.3	8.51

The absorbance at 0 μs of a sample measured in [a] vacuum and [b] methanol vapor. [c] An α-phase Ga_2O_3 sample obtained by calcination of α-Ga_2O_3 at 673 K; [d] A β-phase Ga_2O_3 sample obtained by calcination of α-Ga_2O_3 at 1073 K; [e] A Ga_2O_3 sample with α–β phase junctions on the surface; obtained by calcination of α-Ga_2O_3 at 863 K.

photogenerated holes transfer from the β phase to the α phase, driven by the potential difference caused by the differing band levels of α-Ga_2O_3 and β-Ga_2O_3. Although such a potential difference is small, it can still serve as the driving force for efficient charge separation and transfer.[13] As a result, the photogenerated electrons and holes can be spatially separated into two different phases and thus charge recombination is drastically inhibited, which is of great benefit for enhancing activity in the photocatalytic reaction.

In summary, the photocatalytic activity of Ga_2O_3 for water splitting has been found to be related to its surface structure, and can be significantly enhanced by tailored α–β phase junctions on the surface. The enhanced photocatalytic performance has been shown to be due to efficient charge separation and transfer across the α–β phase junction. Simultaneous exposure of both phases in the outer region is crucial for the fulfillment of the phase junction function in charge separation. As polymorphic semiconductors are quite common in nature, an atomically well-matched phase junction can be conveniently fabricated by fine-tuning the phase transformation conditions. The phase-junction approach described here will open new avenues for the development of efficient photocatalysts for overall water splitting, as well as photoelectronic devices.

Experimental Section

Preparation of Ga_2O_3 and photocatalytic reactions: α-Ga_2O_3 was prepared by the precipitation method. Other samples were prepared by calcining an α-Ga_2O_3 sample for 1.5 h at elevated temperatures (from 673 K to 1073 K). Photocatalytic overall water splitting reactions were performed in an inner irradiation reaction vessel connected to a closed circulation system under 450 W high-pressure mercury lamp irradiation. A NiO_x (2 wt%) co-catalyst was loaded onto the Ga_2O_3 samples. The evolved gases were analyzed by an on-line gas chromatograph.

Time-resolved spectroscopy: The powdered Ga_2O_3 was dispersed on a CaF_2 plate for measurement. Transient absorption measurements were carried out in an air atmosphere, and time-resolved FT-IR was carried out in a quartz cell equipped with BaF_2 windows. The IR cell was connected to the vacuum system, which can be used to introduce water or methanol vapor into the cell. Before each run of the experiment at room temperature, the system was thoroughly evacuated. Detailed procedures can be found in the Supporting Information.

Received: September 18, 2012
Published online: November 19, 2012

Keywords: charge transfer · gallium oxide · phase junctions · photocatalysis · water splitting

[1] K. Maeda, K. Teramura, D. L. Lu, T. Takata, N. Saito, Y. Inoue, K. Domen, *Nature* **2006**, *440*, 295 – 295; H. G. Kim, D. W. Hwang, J. S. Lee, *J. Am. Chem. Soc.* **2004**, *126*, 8912 – 8913; M. Grätzel, *Nature* **2001**, *414*, 338 – 344; X. B. Chen, L. Liu, P. Y. Yu, S. S. Mao, *Science* **2011**, *331*, 746 – 750.

[2] A. Kudo, Y. Miseki, *Chem. Soc. Rev.* **2009**, *38*, 253 – 278; F. E. Osterloh, *Chem. Mater.* **2008**, *20*, 35 – 54.

[3] K. Maeda, A. Xiong, T. Yoshinaga, T. Ikeda, N. Sakamoto, T. Hisatomi, M. Takashima, D. Lu, M. Kanehara, T. Setoyama, T. Teranishi, K. Domen, *Angew. Chem.* **2010**, *122*, 4190 – 4193; *Angew. Chem. Int. Ed.* **2010**, *49*, 4096 – 4099.

[4] O. Khaselev, J. A. Turner, *Science* **1998**, *280*, 425 – 427; A. J. Nozik, *Appl. Phys. Lett.* **1976**, *29*, 150 – 153.

[5] H. G. Kim, P. H. Borse, W. Choi, J. S. Lee, *Angew. Chem.* **2005**, *117*, 4661 – 4665; *Angew. Chem. Int. Ed.* **2005**, *44*, 4585 – 4589; J. Zhang, Q. Xu, Z. Feng, M. Li, C. Li, *Angew. Chem.* **2008**, *120*, 1790 – 1793; *Angew. Chem. Int. Ed.* **2008**, *47*, 1766 – 1769; X. Zong, H. J. Yan, G. P. Wu, G. J. Ma, F. Y. Wen, L. Wang, C. Li, *J. Am. Chem. Soc.* **2008**, *130*, 7176 – 7177.

[6] R. Roy, V. G. Hill, E. F. Osborn, *J. Am. Chem. Soc.* **1952**, *74*, 719 – 722.

[7] F. T. Fan, Z. C. Feng, C. Li, *Acc. Chem. Res.* **2010**, *43*, 378 – 387; M. J. Li, Z. H. Feng, G. Xiong, P. L. Ying, Q. Xin, C. Li, *J. Phys. Chem. B* **2001**, *105*, 8107 – 8111; M. J. Li, Z. C. Feng, P. L. Ying, Q. Xin, C. Li, *Phys. Chem. Chem. Phys.* **2003**, *5*, 5326 – 5332; J. Zhang, M. J. Li, Z. C. Feng, J. Chen, C. Li, *J. Phys. Chem. B* **2006**, *110*, 927 – 935.

[8] R. Rao, A. M. Rao, B. Xu, J. Dong, S. Sharma, M. K. Sunkara, *J. Appl. Phys.* **2005**, *98*, 094312.

[9] D. Machon, P. F. McMillan, B. Xu, J. Dong, *Phys. Rev. B* **2006**, *73*, 094125.

[10] Y. B. Lou, X. B. Chen, A. C. Samia, C. Burda, *J. Phys. Chem. B* **2003**, *107*, 12431 – 12437.

[11] A. Othonos, M. Zervos, C. Christofides, *J. Appl. Phys.* **2010**, 108, 124302.

[12] T. Chen, Z. H. Feng, G. P. Wu, J. Y. Shi, G. J. Ma, P. L. Ying, C. Li, *J. Phys. Chem. C* **2007**, *111*, 8005 – 8014; A. Yamakata, T. Ishibashi, H. Onishi, *J. Phys. Chem. B* **2002**, *106*, 9122 – 9125; T. L. Thompson, J. T. Yates, *Chem. Rev.* **2006**, *106*, 4428 – 4453.

[13] J. Pan, G. Liu, G. Q. Lu, H.-M. Cheng, *Angew. Chem.* **2011**, *123*, 2181 – 2185; *Angew. Chem. Int. Ed.* **2011**, *50*, 2133 – 2137; R. Hengerer, L. Kavan, P. Krtil, M. Gratzel, *J. Electrochem. Soc.* **2000**, *147*, 1467 – 1472.